

## Numerical simulation of effect of non-spherical particle shape and bed size on hydrodynamics of packed beds

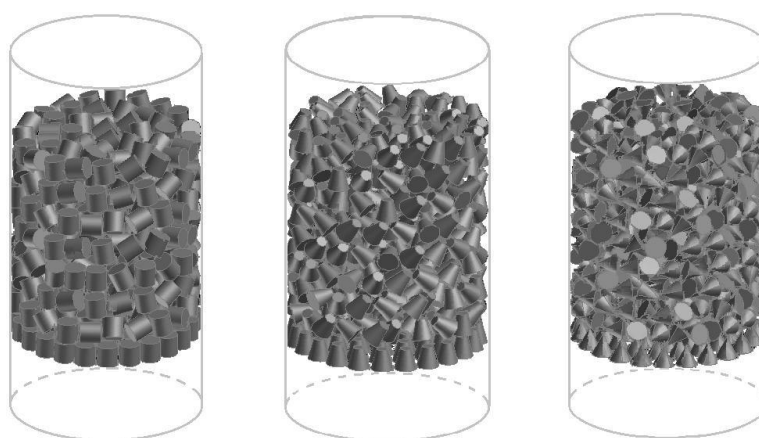
Saeid Mohammadmahdi, Ali Reza Miroliaei\*

Department of Chemical Engineering, University of Mohaghegh Ardabili, Ardabil, Iran

### HIGHLIGHTS

- Flow channelling and vortex flow depend on particle shape, fluid velocity and bed porosity.
- The pressure drop of fluid with truncated cone particles is lower than the cone and cylindrical particles.
- Stationary points with cylindrical particles are more than the other particles.
- Vortex flow increases the pressure drop of fluid.

### GRAPHICAL ABSTRACT



### ARTICLE INFO

#### Article history:

Received 8 August 2017

Revised 20 October 2017

Accepted 22 October 2017

#### Keywords:

Flow channelling

Non-spherical particles

Pressure drop

Porosity

Vortex flow

### ABSTRACT

Fluid flow has a fundamental role in the performance of packed bed reactors. Some related issues, such as pressure drop, are strongly affected by porosity, so non-spherical particles are used in industry for enhancement or creation of the desired porosity. In this study, the effects of particle shape, size, and porosity of the bed on the hydrodynamics of packed beds are investigated with three non-spherical particles namely cylindrical, cone, and truncated cone in laminar and turbulent flow regimes ( $15 \leq Re \leq 2500$ ) using computational fluid dynamics. According to results obtained from the simulations, it was observed that flow channeling occurs in the parts of the bed that are not well covered by particles, which is more near the wall. CFD simulations showed that the vortex flow around the cylindrical particles is more than the cone and truncated cone particles and are caused by increasing the pressure drop of fluid in the bed. It was also found that the particles creating less porosity in the bed, due to their shape, are caused by increasing the pressure drop of fluid. The numerical results showed good agreement with available empirical correlations in the literature.

\* Corresponding author: Tel.: +9845-33512910 ; Fax: +9845-33512904 ; E-mail address: [armiroliaei@uma.ac.ir](mailto:armiroliaei@uma.ac.ir)

DOI: 10.22104/JPST.2017.2397.1093

## 1. Introduction

There are several processes in industries, such as chemical, petrochemical and refinery industries, which require packed bed contactors and reactors. A packed bed is usually a hollow tube filled with layers of catalyst particles. The particles in the bed can be different shapes such as spherical, cylindrical, cubic, cone, truncated cone, etc. In many cases, non-spherical particles are selected due to the operating conditions and suitable distribution of fluid in the bed. Figure 1 shows a packed bed with spherical particles. Since packed beds are designed for interaction and increasing collision between materials, hydrodynamics and its related issues such as pressure drop of fluid, flow regimes and some of the incoming forces on the particles have an essential role in the performance of packed bed reactors. In fact, pressure drop of fluid in packed beds is strongly influenced by porosity, and for this reason non-spherical particles are used in industries to create the desired porosity. Due to safety and economic conditions, bed to particle diameter ratio of packed bed is also selected in the ranges of  $3 < N = D/d_p < 8$  [1,2].

There are many numerical and experimental studies on the hydrodynamics of packed beds with the spherical particles. For example, the pressure drop and drag coefficient in square channels were studied by Calis *et al.* [3]. Their results showed good agreement with LDA measurements. Atmakidis and Kenig [4] investigated the wall effect on pressure drop in packed beds. They compared the CFD results with the empirical correlations of Zhavoronkov *et al.* and Reichelt. Reddy and Joshi [5] investigated CFD modeling of pressure drop and

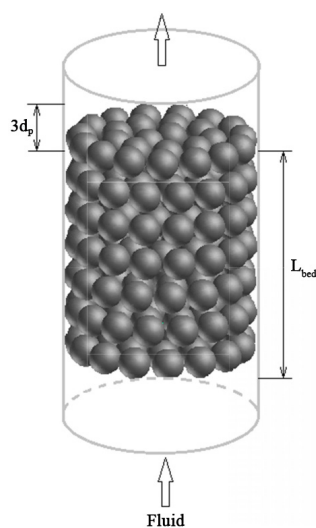


**Fig. 1.** Schematic of a packed bed with spherical particles.

drag coefficient in fixed beds with spherical particles. They stated that drag coefficient obtained from the CFD simulations become closer to the empirical equation of Ergun as the bed to particle diameter ratio increased due to reducing the effects of wall friction. The shape effects on the packing density of frustums were studied by Zhao *et al.* [6]. Their studies showed that the optimal aspect ratio of truncated cones is 0.8 and increases as the radii ratio increases. Also, they proposed a correlation between the packing density and shape parameters. Allen *et al.* [7] studied the effects of particle shape, size distribution, packing arrangement and roughness of particles on the packed bed pressure drop. Their results showed that the particle shape, packing arrangement and surface roughness of particles affect the pressure drop. Rong *et al.* [8] investigated fluid flow in packed beds with different spheres using a parallel lattice-Boltzmann model. The effects of size ratio and volume fraction on the fluid flow and drag force were studied. Their results showed that the dispersion of particles affects flow distribution and fluid-particle interaction forces. Also, they suggested a correlation to calculate the drag force. Experimental study and numerical simulation of pressure drop in a packed bed with arbitrarily shaped particles were carried out by Vollmari *et al.* [9]. They indicated that simulations are in good agreement with experiments depending on the particle shape and size and is often better in comparison with empirical correlations. Bu *et al.* [10] considered the flow transitions in three different structured packed beds, such as simple cubic, body center cubic and face center cubic packing forms, using electrochemical techniques. They observed three different flow regimes in the packed beds, i.e. laminar, transition and turbulent flow regimes. Also, they explained that flow regimes in packed beds depend on the arrangement of the particles. Du *et al.* [11] studied the porosity and pressure drop in packed beds experimentally and statistically. Their analysis showed that the experimental data and the predicted equation for particles with different sizes have good agreement together. Pressure drop in slender packed beds was investigated by Guo *et al.* [12]. They found that pressure drop in packed beds depends on the bed structure, as a minor change in the bed structure creates a notable pressure drop even though the beds have the same porosity.

In this research, the effects of particle shape and bed size on pressure drop of fluid in packed beds with non-

spherical particles such as cylindrical, cone, and truncated cone particles are investigated to achieve a suitable distribution of fluid flow and lower pressure drop in the bed. The validation of the CFD simulation results is carried out with proposed empirical correlations in the literature.

## 2. Empirical correlations for pressure drop prediction in packed beds with non-spherical particles

The empirical equation of Ergun [13] is used to predict the pressure drop in the packed beds with spherical particles. This correlation is applicable in a wide range of flow regimes. The estimated pressure drop according to Ergun equation depends on the properties of the bed and fluid such as bed porosity and particle diameter, fluid flow rate, viscosity and density of fluid as follows:

$$\frac{\Delta P}{L} = \frac{150\mu(1-\varepsilon)^2}{\varepsilon^3 d_p^2 \phi^2} u_s + \frac{1.75(1-\varepsilon)\rho}{\varepsilon^3 d_p \phi} u_s^2 \quad (1)$$

In above equation  $\mu$  and  $\rho$  are the dynamic viscosity and density of fluid,  $u_s$  is the superficial velocity of fluid,  $\varepsilon$  is the porosity of bed,  $d_p$  and  $\phi$  are the diameter and sphericity of particles, respectively.

The sphericity of particles is defined as the ratio between the surface area of the volume equivalent sphere and the surface area of the particle:

$$\phi = \left[ 36\pi \cdot \frac{V_p^2}{A_p^3} \right]^{\frac{1}{3}} \quad (2)$$

The correction of Ergun equation for non-spherical particles has been carried out by some researchers. Some of these relations are shown in Table 1.

The coefficients of (3) and (7) equations have been mentioned in Tables 2 and 3, respectively.

**Table 2.** Coefficients in equation (3) [10].

Particle shape	$K_1$	$k_1$	$k_2$
Cylindrical	190	2	0.77
All particles	155	1.43	0.83

**Table 3.** Coefficients in equation (7) [6].

Particle shape	a	b	c
Cubic	240	10.8	0.1
Cylindrical	216	8.8	0.12

## 3. CFD modeling

### 3.1. Characteristics of particles and beds

Packed beds were designed with three different particles types, of cylindrical, cone, and truncated cone, in different ratios of low bed to particle diameter. It was assumed that the size of particles is constant and the parameters of A and B were also defined for the dimensions of particles. A is the ratio of the height of the particles to the larger particle's diameter ( $A=L_p/d_p$ ), and B is the ratio of the smaller particle's diameter to larger particle's diameter ( $B=d/d_p$ ). Therefore, the values of A and B for the cylindrical, cone, and truncated cone particles are A=1 and B=1, A=1 and B=0, and A=1 and

**Table 1.** Empirical correlations for calculating pressure drop with non-spherical particles.

$$\text{Eisfeld and Schnitzlein [10]} \quad \frac{\Delta P}{L} = K_1 \frac{\mu_f(1-\varepsilon)^2}{\varepsilon^3 d_p^2} u_s M^2 + \frac{(1-\varepsilon)\rho_f}{\varepsilon^3 d_p} u_s^2 \frac{M}{B_w} \quad (3)$$

$$M = 1 + \frac{4d_{pe}}{6D(1-\varepsilon)}, \quad B_w = \left[ k_1 \left( \frac{d_p}{D} \right)^2 + k_2 \right]^2 \quad (4)$$

$$\text{Nemec and Levec [11]} \quad \frac{\Delta P}{L} = \frac{150\mu(1-\varepsilon)^2}{\varepsilon^3 d_{sv}^2 \phi^{3/2}} u_s + \frac{1.75(1-\varepsilon)\rho}{\varepsilon^3 d_{sv} \phi^{4/3}} u_s^2 \quad (5)$$

$$\text{Singh et al. [12]} \quad \frac{\Delta P}{L} = 4.4666 \cdot \left( \frac{\rho_f \cdot u_s \cdot d_e}{\mu_f} \right)^{-0.2} \cdot \varepsilon^{-2.945} \cdot \phi^{0.696} \cdot e^{11.85(\log \phi)^2} \cdot \frac{\rho_f \cdot u_s^2}{d_e} \quad (6)$$

$$\text{Allen et al. [6]} \quad \frac{\Delta P}{L} = \left[ \frac{a}{\text{Re}_{\text{Duct}}} + \frac{b}{\text{Re}_{\text{Duct}}^c} \right] \cdot \frac{(1-\varepsilon)}{\varepsilon^3} \cdot \frac{\rho_f \cdot u_s^2}{8} \cdot \frac{\sum A_p}{\sum V_p} \quad (7)$$

$$\text{Re}_{\text{Duct}} = \frac{4 \cdot \rho_f \cdot u_s^2 \cdot \sum V_p}{\mu_f \cdot (1-\varepsilon) \cdot \sum A_p} \quad (8)$$

B=0.5, respectively. Table 4 describes the characteristics of the particles and the beds.

The geometry of designed beds with the different shapes are shown in Figure 2.

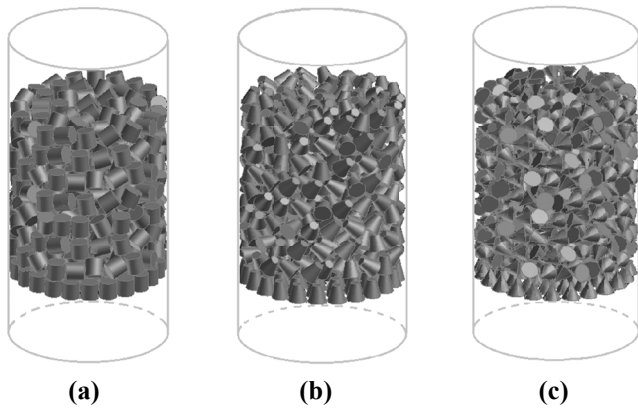


**Fig. 2.** Geometry of designed beds: (a) packed bed with cylindrical particles, (b) packed bed with truncated cone particles, and (c) packed bed with cone particles.

3.2. Governing equations

Momentum and continuity equations are used in order to investigate fluid flow through the packed beds. The continuity equation is defined as follows [2]:

$$\frac{\partial \rho}{\partial t} + \nabla \cdot (\rho u) = S_m \tag{9}$$

$S_m$  is the source term that is equal to zero in our simulations.

The equation for conservation of momentum is:

$$\frac{\partial(\rho u)}{\partial t} + \nabla \cdot (\rho u u) = -\nabla p + \nabla \cdot (\rho(\vartheta + \vartheta_t)\nabla u) + \rho g_i \tag{10}$$

In the above balance  $\rho g_i$  is the gravitational force.  $\vartheta$  and  $\vartheta_t$  are the kinetic viscosity in laminar and turbulent flow regimes, respectively. The kinetic viscosity in the turbulent flow regime depends on two parameters, i.e. turbulent kinetic energy,  $k$ , and dissipation rate,  $\epsilon$ .

The RNG  $k-\epsilon$  model was used in the turbulent flow regime [17]. The parameters of this model are calculated from the following transport equations:

$$\frac{\partial(\rho k)}{\partial t} + \nabla \cdot (\rho k u) = \rho \vartheta_t (\nabla u)^2 + \nabla \cdot (\rho \alpha_k \vartheta_t \nabla k) - \rho \epsilon \tag{11}$$

$$\frac{\partial(\rho \epsilon)}{\partial t} + \nabla \cdot (\rho \epsilon u) = \nabla \cdot (\rho \alpha_\epsilon \vartheta_t \nabla \epsilon) + C_{1\epsilon} \frac{\epsilon}{k} \rho \vartheta_t (\nabla u) - C_{2\epsilon} \rho \frac{\epsilon^2}{k} - R_\epsilon \tag{12}$$

In these equations,  $C_{1\epsilon}$  and  $C_{2\epsilon}$  are equal to 1.48 and 1.68, respectively. Also,  $\alpha_k = \alpha_\epsilon = 1.393$ ,  $\vartheta_t$  and  $R_\epsilon$  are defined as follows:

$$\vartheta_t = C_\mu \frac{k^2}{\epsilon} \tag{13}$$

$$R_\epsilon = \frac{C_\mu \rho \eta^3 (1 - \eta / \eta_0) \epsilon^2}{1 + \beta \eta^3} \tag{14}$$




Here,  $C_\mu = 0.0845$ ,  $\eta = Sk / \epsilon$ ,  $\eta_0 = 4.38$  and  $\beta = 0$ .

$S$  is the modulus of the mean rate-of-strain tensor:

$$S = \sqrt{S_{ij} S_{ij}} \tag{15}$$

The finite volume method, ANSYS FLUENT software, was chosen for solving momentum and

**Table 4.** Characteristics of particles and beds.

Particle shape	Dimension (mm)			Particle volume (mm <sup>3</sup> )×10 <sup>-2</sup>	Sphericity	Bed volume (mm <sup>3</sup> )×10 <sup>-5</sup>	Porosity	N= D/d <sub>sv</sub>
	L <sub>p</sub>	d <sub>p</sub>	d					
	23	23	23	95.56	0.87	8.34	0.576	4.17
	23	23	23	95.56	0.87	28.1	0.625	6.26
	23	23	23	95.56	0.87	94.4	0.602	9.39
	23	23	11.5	55.74	0.84	8.34	0.722	4.36
	23	23	11.5	55.74	0.84	28.1	0.699	6.54
	23	23	11.5	55.74	0.84	94.4	0.708	9.82
	23	23	0	31.85	0.77	8.34	0.710	5.24
	23	23	0	31.85	0.77	28.1	0.741	7.86
	23	23	0	31.85	0.77	94.4	0.748	11.80

continuity equations. The air was assumed as the fluid through the packed beds in the simulations. The boundary conditions are as follows:

- Steady state flow;
- Incompressible fluid;
- Constant velocity in the bed inlet;
- Constant pressure (1 atm) in the bed outlet; and
- Non-slip condition for the walls and the surface of particles.

The SIMPLE algorithm was used for coupling velocity and pressure. Second order upwind discretization method was also applied to increase the accuracy of the results. The convergence criterion was maintained to achieve a very low level of the residual, about  $10^{-5}$  in all equations.

## 4. Results and discussion

### 4.1. Mesh generation

The most important step in the simulation is mesh generation. In fact, mesh geometry should be designed in such a way that changing a number of meshes doesn't affect results, and the geometry must be independent of the mesh. For example, a grid independence study with unstructured tetrahedral mesh was carried out in the packed bed with cylindrical particles of  $N = 6.26$  with five different mesh sizes, i.e. 5, 4, 3, 2.5 and 2 mm. The pressure drop was evaluated for different mesh sizes and the optimum mesh was selected. It was observed that the pressure drop varies from 8.7%, 5.9%, 3.2% and 0.29% when the grid size is changed from 5 to 4, 4 to 3, 3 to 2.5 and 2.5 to 2 mm, respectively. As it can be seen from Table 5, in the grid size 2.5 mm the pressure drop is independent of mesh size. Therefore, the grid size of 2.5 mm was selected for our simulations of a packed bed with cylindrical particles. The results of the mesh independence study for cylindrical, truncated cone, and

**Table 5.** Grid independence results for a packed bed with cylindrical particles in  $N=6.26$ .

Mesh size (mm)	5	4	3	2.5	2
$\Delta P \times 10^{-3}$ (pa)	8.54	9.36	9.95	10.28	10.31
Pressure drop variations		8.7%			
			5.9%		
				3.2%	
					0.29%

cone have been stated in Tables 5, 6 and 7, respectively.

**Table 6.** Grid independence results for packed bed with truncated cone particles in  $N=6.54$ .

Mesh size (mm)	4	3.5	3	2.5	2
$\Delta P \times 10^{-3}$ (pa)	7.16	7.79	8.06	8.23	8.37
Pressure drop variations		7.98%			
			3.38%		
				2.1%	
					1.65%

**Table 7.** Grid independence results for a packed bed with cone particles in  $N=7.86$ .

Mesh size (mm)	4	3.5	3	2.5	2
$\Delta P \times 10^{-3}$ (pa)	6.61	7.81	8.92	9.10	9.78
Pressure drop variations		15.36%			
			12.4%		
				1.9%	
					6.9%

### 4.2. Velocity profiles

Velocity profiles in the packed beds with cylindrical, cone, and truncated cone particles and a bed volume of  $94.9 \times 10^5 \text{ mm}^3$  in the turbulent flow regime have been shown as contour and vector in Figures 3 and 4. As shown in these figures, when the fluid enters the packed bed it passes through a porous media created by the particles. From velocity contours in Figure 3, it is known that in the special regions of the bed where the distance between the particle-particle and particle-wall is low, the fluid velocity increases because of a lower passing surface for fluid flow. It is also seen that the channeling phenomenon occurs in the parts of the bed that are not well covered by particles. On the other hand, the flow channeling was observed more near the wall.

After the collision of the fluid with particles in the bed the fluid velocity decreases (see Figure 3) and the region where the fluid velocity is close to zero is called the stationary point. The stationary points were seen more in the packed beds with cylindrical particles.

As it is shown in Figure 4, a vortex flow is created in the bed. It occurs in areas that particles are close each other. The vortex flow was also observed in parts of the bed outlet. This type of flow was seen less in the packed beds with the cone and truncated cone particles because



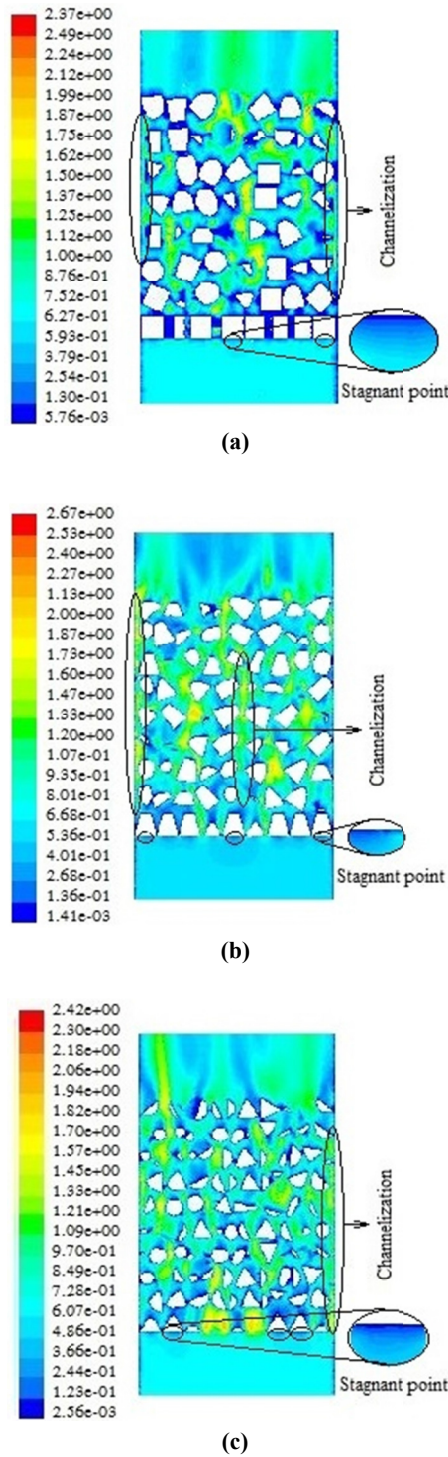


**Fig. 3.** Velocity contour in the packed beds with  $V_b = 94.9 \times 10^5 \text{ mm}^3$  and  $V_f = 0.5 \text{ m/s}$ : a) cylindrical particles, b) truncated cone particles, and c) cone particles.

of the shape and surface of these particles.

Some of the most important parameters causing the turbulent flow in packed beds include particle shape, fluid velocity and bed porosity. So the characteristics of flow, such as flow channeling and vortex flow, can affect the pressure drop of fluid into the bed which will be discussed in the following sections.

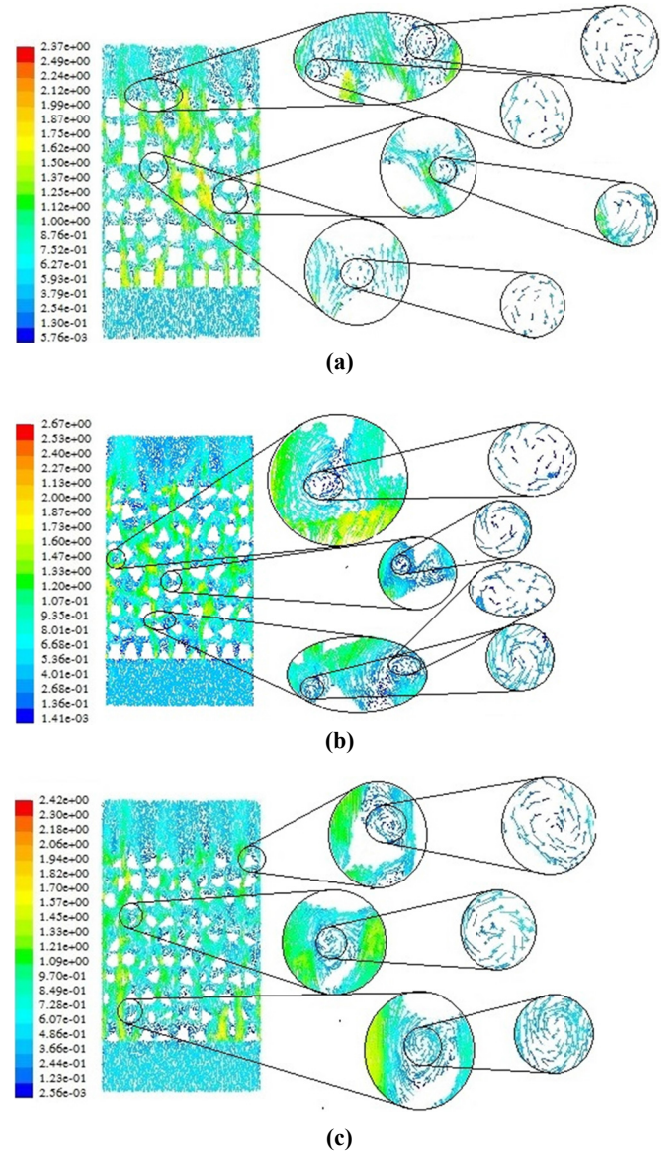


**Fig. 4.** Velocity vectors in the packed beds with  $V_b = 94.9 \times 10^5 \text{ mm}^3$  and  $V_f = 0.5 \text{ m/s}$ : a) cylindrical particles, b) truncated cone particles, and c) cone particles.

### 4.3. Pressure drop

Pressure drop in packed beds is the most important parameter as the heat and mass transfer are strongly relevant to pressure drop. Therefore, study of effective parameters on pressure drop in packed beds is required. The CFD obtained pressure drop results for cylindrical, cone, and truncated cone particles in laminar and turbulent flow regimes are shown in Figures 5, 6 and 7, respectively. The validation of the CFD simulations was carried out with empirical correlations of Einfeld and Schnitzlein [14], Nemeč and Levec [15], and Allen *et al.* [7]. As it can be seen in these figures, increasing both length and diameter of the beds caused increasing pressure drop of fluid in the bed because the fluid needs

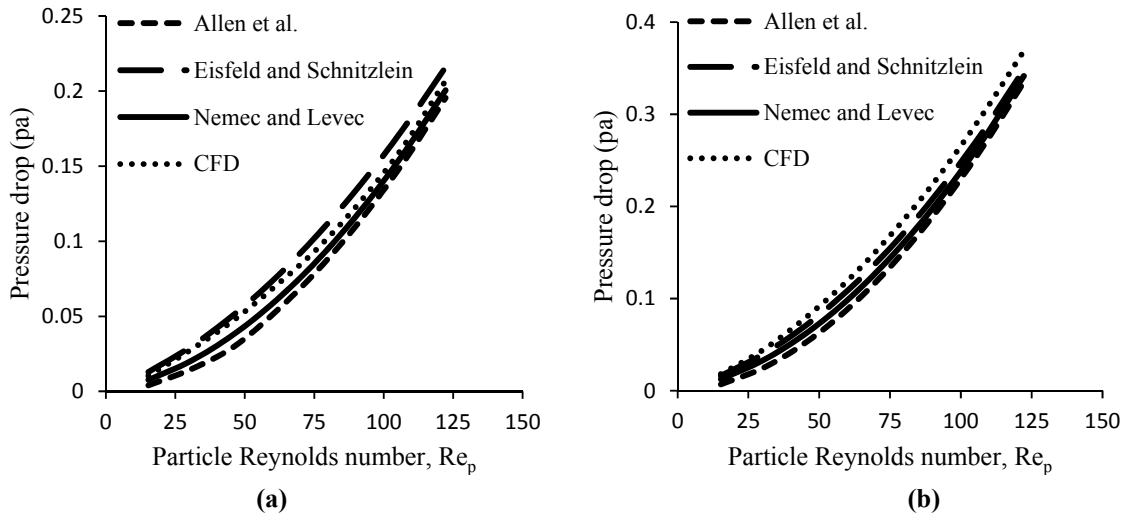


**Fig. 5.** Comparison of CFD pressure drop with empirical correlations for the packed bed with cylindrical particles in laminar flow: a)  $N=4.17$  and b)  $N=9.39$ .

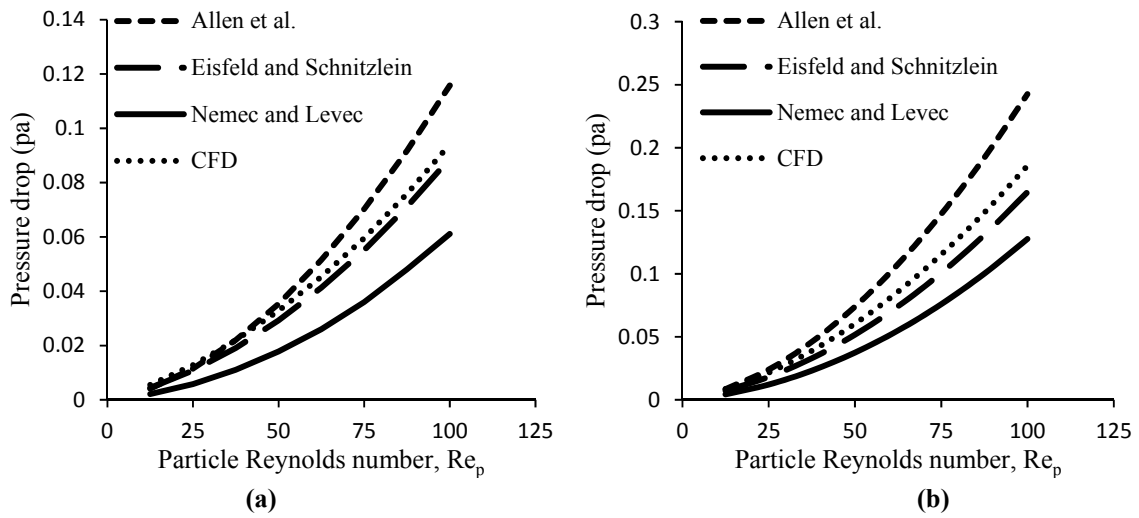


**Fig. 6.** Comparison of CFD pressure drop with empirical correlations for the packed bed with cone particles in laminar flow: a)  $N=5.24$  and b)  $N=11.8$ .

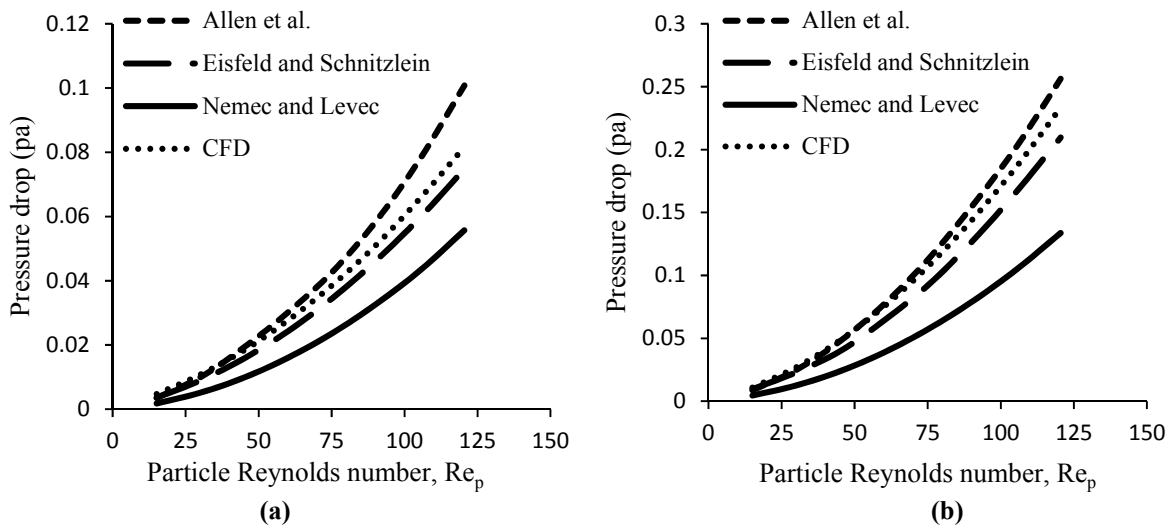


**Fig. 7.** Comparison of CFD pressure drop with empirical correlations for the packed bed with truncated cone particles in laminar flow: a)  $N=4.36$  and b)  $N=9.82$ .

to pass a longer path in the bed. It is also observed that the pressure drop of fluid at the same Reynolds number for the truncated cone particles is lower than the cone and cylindrical particles.

Comparison of CFD pressure drop variations and empirical correlations in the turbulent flow regime for packed beds with different particles is carried out in Figures 8, 9 and 10, respectively. As mentioned before, the pressure drop values for cylindrical particles are more than the cone and truncated cone particles because of the eddy and vortex flows.

4.4. Effect of bed porosity on the pressure drop

The porosity of the bed is one of the parameters that most affects the pressure drop of fluid. A comparison between created pressure drop in the packed beds with cylindrical, cone, and truncated cone particles at

different ratios of bed to particles diameter, according to Table 4, is shown in Figures 11 and 12. As seen in these figures, the pressure drop variations of fluid in the packed bed with cylindrical particles are more than the cone and truncated cone particles. It is also observed that the pressure drop of fluid in the packed beds with cone and truncated cone particles are close each other. The main reason for the pressure drop in the beds with different types of particles is that the bed porosity is created according to the shape of the particles. As can be seen in Figures 11 and 12, the pressure drop in the beds increases as the porosity of the bed decreases because as the porosity of the bed decreases the fluid passes through a more twisted path into the bed which causes the pressure drop of fluid to increase. It is also known that the particles having lower porosity, e.g. cylindrical particles, create more pressure drop in the bed.

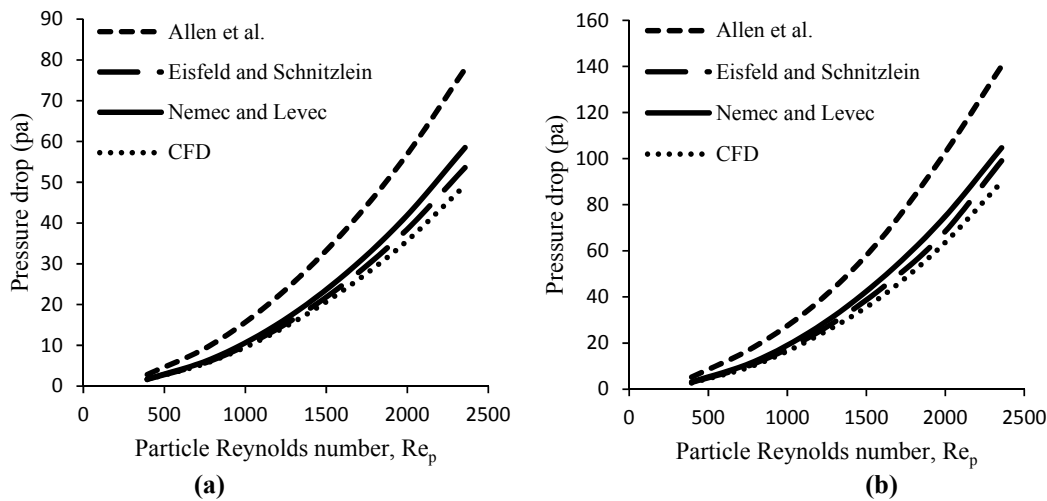


Fig. 8. Comparison of CFD pressure drop with empirical correlations for the packed bed with cylindrical particles in turbulent flow: a)  $N=6.26$  and b)  $N=9.39$ .

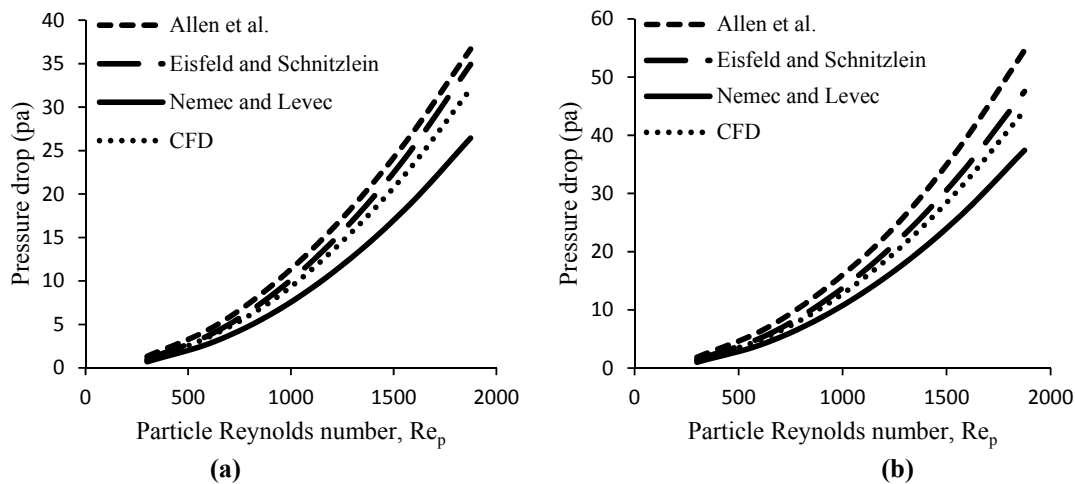
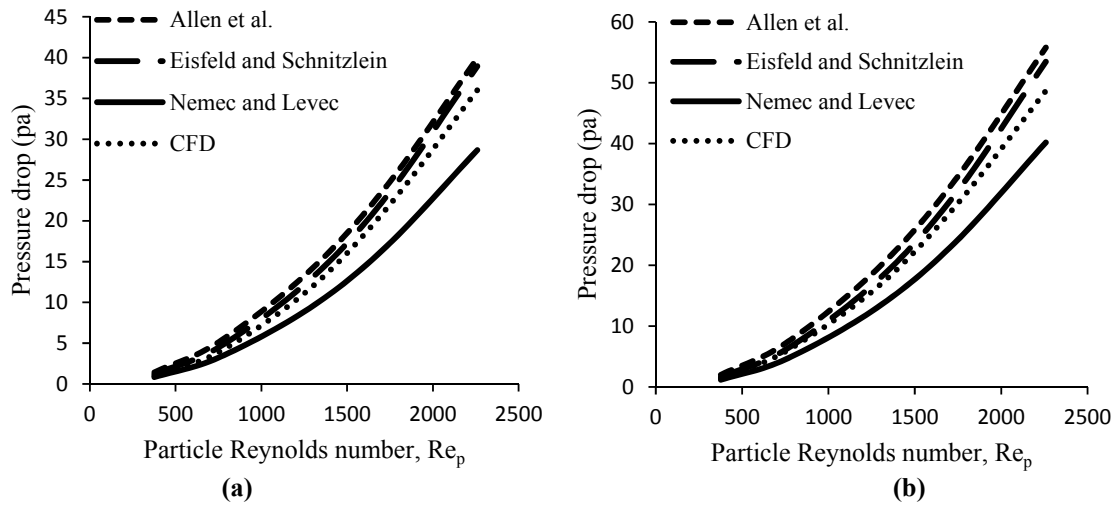
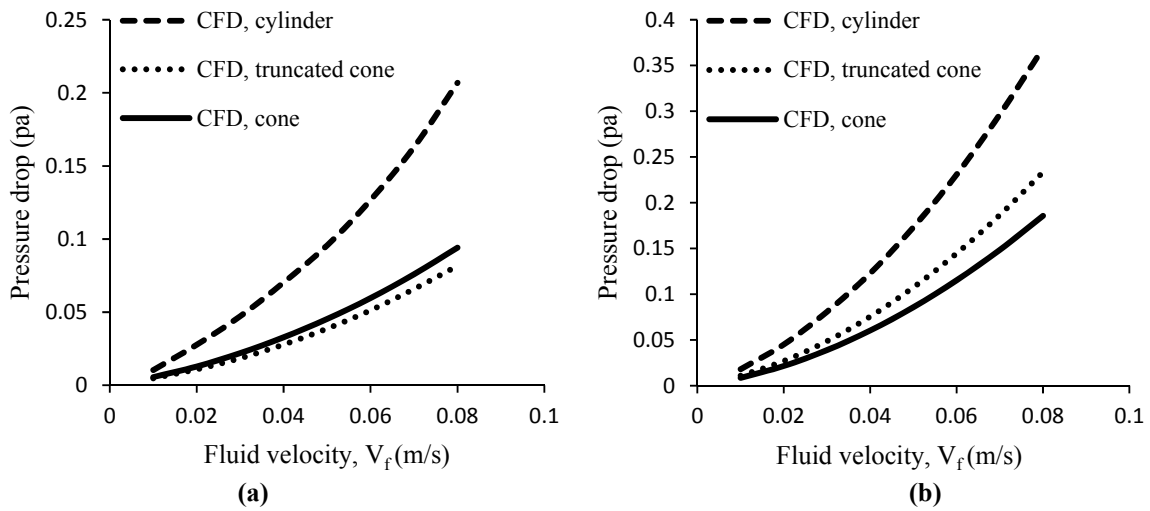


Fig. 9. Comparison of CFD pressure drop with empirical correlations for the packed bed with cone particles in turbulent flow: a)  $N=7.82$  and b)  $N=11.8$ .





**Fig. 10.** Comparison of CFD pressure drop with empirical correlations for the packed bed with truncated cone particles in turbulent flow: a)  $N=6.52$  and b)  $N=9.82$ .



**Fig. 11.** Pressure drop variations vs. fluid velocity for cylindrical, truncated cone, and cone particles in a laminar flow regime: a)  $V_b = 8.34 \times 10^5 \text{ mm}^3$  and b)  $V_b = 94.9 \times 10^5 \text{ mm}^3$ .

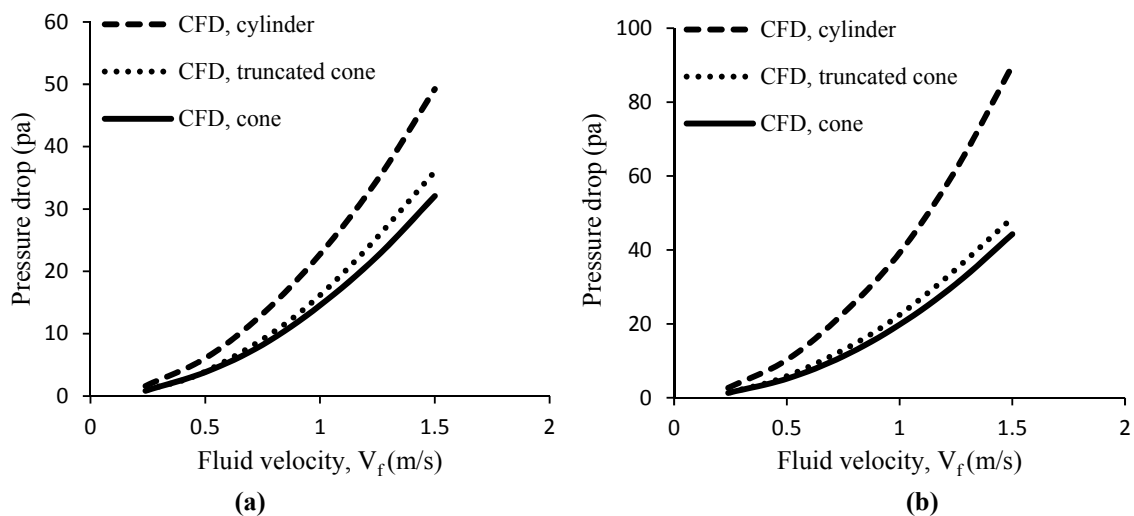


**Fig. 12.** Pressure drop variations vs. fluid velocity for cylindrical, truncated cone and cone particles in a turbulent flow regime: a)  $V_b = 8.34 \times 10^5 \text{ mm}^3$  and b)  $V_b = 94.9 \times 10^5 \text{ mm}^3$ .

## 5. Conclusion

In this study, characteristics of fluid flow, such as flow channeling and vortex flow, and the effect of particle shape on the pressure drop of fluid in packed beds with a low bed to particle diameter ratio were investigated. Three types of particles cylindrical, cone, and truncated cone were selected. The CFD simulation results were validated using empirical correlations from the literature. According to the contours and vectors of fluid flow in all beds, it was seen that the channeling phenomenon occurs in some regions of the bed because of inadequate cover between particles and particle-wall. It was also observed that vortex flow with cylindrical particles is more than the cone and truncated cone particles. As result, we found the flow channeling and vortex flow properties of fluid flow depend on the shape of particles, fluid velocity and bed porosity.

Numerical results showed that the pressure drop of fluid in the packed bed with truncated cone particles is lower than the cylindrical and cone particles. The main reason for the pressure drop of fluid with different particles is the bed porosity, which is created according to the shape of the particles; but in equal porosity conditions pressure drop depends on eddies, vortex flow, and other forces (such as drag force) that are different due to the particle shape. As shown in the simulation results, the RNG k- $\epsilon$  model is appropriate for simulation and provides acceptable results in a turbulent flow regime.

## Nomenclature

$A_p$	Particle surface area (m <sup>2</sup> )
$A_w$	Wall correction term
a, b, c	Constants in Eq. (7)
$B_w$	Wall correction term
D	Bed diameter (m)
$d_p$	Large diameter of particle (m)
D	Small diameter of particle (m)
$d_{sv}$	Equivalent surface volume diameter, $d_{sv}=6.V_p/A_p$ (m)
G	Gravitational acceleration (m/s <sup>2</sup> )
$K_1$	Constant in Eq. (3)
$k_1, k_2$	Constants in Eq. (4)
$L_p$	Length of particles (m)
L	Length of bed (m)

M	Wall correction term
N	Bed to particle diameter ratio, $N=D/d_{sv}$
$n_p$	Number of particles in the bed
$Re_{duct}$	Duct Reynolds number, $Re_{duct} = \frac{2 \cdot \rho \cdot u_s \cdot d_p}{3 \cdot \mu (1-\epsilon)}$
$Re_p$	Particle Reynolds number, $Re_p = \frac{\rho \cdot u_s \cdot d_p}{\mu}$
$u_s$	Superficial velocity (m/s)
$V_p$	Particle volume (m <sup>3</sup> )
$V_b$	Bed volume (m <sup>3</sup> )

## Greek symbols

$\Delta P$	Pressure drop (Pa)
$\epsilon$	Porosity, $\epsilon = 1 - \frac{n_p V_p}{V_b}$
$\mu_f$	Fluid dynamic viscosity (kg/m.s)
$\rho_f$	Fluid density (kg/m <sup>3</sup> )
$\phi$	Particle sphericity
$\mathcal{G}_t$	Turbulence kinetic viscosity
K	Turbulence kinetic energy
$\epsilon$	Rate of dissipation

## References

- [1] J. Ancheyta, J.A.D. Munoz, M.J. Maceas, Experimental and theoretical determination of the particle size of hydrotreating catalysts of different shapes, *Catal. Today*, 109 (2005) 120-127.
- [2] A.G. Dixon, M. Nijemeisland, E.H. Stitt, Packed tubular reactor design using computational fluid dynamics, *Adv. Chem. Eng.* 3 (2006) 307-389.
- [3] H.P.A. Calis, J. Nijenhuis, B.C. Paikert, F.M. Dautzenberg, C.M. van den Bleek, CFD modelling and experimental validation of pressure drop and flow profile in a novel structured catalytic reactor packing, *Chem. Eng. Sci.* 56 (2001) 1713-1720.
- [4] T. Atmakidis, E.Y. Kenig, CFD-based analysis of the wall effect on the pressure drop in packed beds with moderate tube/particle diameter ratios in the laminar flow regime, *Chem. Eng. J.* 155 (2009) 404-410.
- [5] R.K. Reddy, J. B. Joshi, CFD modeling of pressure drop and drag coefficient in fixed beds: Wall effects, *Particuology*, 8 (2010) 37-43.
- [6] J. Zhao, S. Li, P. Lu, L. Meng, T. Li, H. Zhu, Shape

- influences on the packing density of frustums, *Powder Technol.* 214 (2011) 500-505.
- [7] K.G. Allen, T.W. von Backstrom, D.G. Kroger, Packed bed pressure drop dependence on particle shape, size distribution, packing arrangement and roughness, *Powder Technol.*, 246 (2013) 590-600.
- [8] L.W. Rong, K.J. Dong, A.B. Yu, Lattice-Boltzmann simulation of fluid flow through packed beds of spheres: Effect of particle size distribution, *Chem. Eng. Sci.* 116 (2014) 508-523.
- [9] K. Vollmari, T. Oschmann, S. Wirtz, H. Kruggel-Emden, Pressure drop investigations in packings of arbitrary shaped particles, *Powder Technol.* 271 (2015) 109-124.
- [10] Sh. Bu, J. Yang, Q. Dong, Q. Wang, Experimental study of flow transitions in structured packed beds of spheres with electrochemical technique, *Exp. Therm. Fluid Sci.* 60 (2015) 106-114.
- [11] W. Du, N. Quan, P. Lu, J. Xu, W. Wei, L. Zhang, Experimental and statistical analysis of the void size distribution and pressure drop validations in packed beds, *Chem. Eng. Res. Des.* 106 (2016) 115-125.
- [12] Z. Guo, Zh. Sun, N. Zhang, M. Ding, J. Wen, Experimental characterization of pressure drop in slender packed bed ( $1 < D/d < 3$ ), *Chem. Eng. Sci.* 173 (2017) 578-587.
- [13] S. Ergun, Fluid flow through packed columns, *Chem. Eng. Prog.* 48 (1952) 89-94.
- [14] B. Eisfeld, K. Schnitzlein, The influence of confining walls on the pressure drop in packed beds, *Chem. Eng. Sci.* 56 (2001) 4321-4329.
- [15] D. Nemeč, J. Levec, Flow through packed bed reactors: 1. Single-phase flow, *Chem. Eng. Sci.* 60 (2005) 6947-6957.
- [16] R. Singh, R.P. Saini, J.S. Saini, Nusselt number and friction factor correlations for packed bed solar energy storage system having large sized elements of different shapes, *Sol. Energy*, 80 (2006) 760-771.
- [17] ANSYS FLUENT 12.0.16, Theory Guide. ANSYS Inc., 2009.